

Can magnetic fields be detected during the inspiral of binary neutron stars?

Bruno Giacomazzo,¹ Luciano Rezzolla^{1,2} and Luca Baiotti³

¹Max-Planck-Institut für Gravitationsphysik, Albert-Einstein-Institut, Potsdam-Golm, 14476, Germany

²Department of Physics and Astronomy, Louisiana State University, Baton Rouge, LA 70803, USA

³Graduate School of Arts and Sciences, University of Tokyo, Komaba, Meguro-ku, Tokyo, 153-8902, Japan

11 November 2018

ABSTRACT

Using accurate and fully general-relativistic simulations we assess the effect that magnetic fields have on the gravitational-wave emission produced during the inspiral and merger of magnetized neutron stars. In particular, we show that magnetic fields have an impact after the merger, because they are amplified by a Kelvin-Helmholtz instability, but *also* during the inspiral, most likely because the magnetic tension reduces the stellar tidal deformation for extremely large initial magnetic fields, $B_0 \gtrsim 10^{17}$ G. We quantify the influence of magnetic fields by computing the overlap, \mathcal{O} , between the waveforms produced during the inspiral by magnetized and unmagnetized binaries. We find that for any realistic magnetic field strength $B_0 \lesssim 10^{14}$ G the overlap during the inspiral is $\mathcal{O} \gtrsim 0.999$ and is quite insensitive to the mass of the neutron stars. Only for unrealistically large magnetic fields like $B_0 \simeq 10^{17}$ G the overlap does decrease noticeably, becoming at our resolutions $\mathcal{O} \lesssim 0.76/0.67$ for stars with baryon masses $M_b \simeq 1.4/1.6 M_\odot$, respectively. Because neutron stars are expected to merge with magnetic fields $\sim 10^8 - 10^{10}$ G and because present detectors are sensitive to $\mathcal{O} \lesssim 0.995$, we conclude that it is very unlikely that the present detectors will be able to discern the presence of magnetic fields during the inspiral of neutron stars.

Key words: relativity – gravitational waves – stars: neutron – binaries: general – magnetic fields – MHD

1 INTRODUCTION

Numerous astronomical observations suggest that large magnetic fields are associated with neutron stars (NSs). Indeed, evidence for the existence of binary NSs is obtained from binary pulsars, in which one or both NSs are seen to have a large magnetic field. In General Relativity such binary systems cannot be stationary because they emit gravitational waves (GWs) which extract energy and angular momentum from the binary, inducing it to inspiral and merge. During the final stages of the inspiral the GW emission is expected to be strong enough to be relevant for the detectors now operative at design sensitivities and it promises to provide important information on the equation of state (EOS) regulating the NS matter (Read et al. 2009). In addition to their importance as sources of GWs, however, the merger of binary NSs is likely to provide important information on the physics of short gamma-ray bursts (GRBs). The coalescence of the two NSs, in fact, gives rise, either promptly or after some interval, to a system composed of a torus orbiting around a rapidly rotating black hole (BH) (Baiotti et al. 2008; Yamamoto et al. 2008). The complex plasma physics

accompanying this event is probably behind the “engine” powering GRBs (Piran 2004; Meszaros 2006).

There is little doubt, therefore, about the importance of assessing the role played by magnetic fields in the inspiral and merger of binary NSs. Yet, determining this accurately is a remarkably difficult task requiring the solution of the Einstein equations together with those of general-relativistic magnetohydrodynamics (GRMHD). So far, only two GRMHD simulations have been reported (Anderson et al. 2008; Liu et al. 2008), reaching different conclusions about the importance of very strong magnetic fields ($B \sim 10^{16} - 10^{17}$ G). The aim of this Letter is to go beyond these qualitative estimates and provide a first quantitative measurement of the influence of magnetic fields on both the inspiral and the merger of magnetized NSs.

By considering a large range of magnetic fields, which includes values more realistic than those used in the works cited above, and two different masses, we find that magnetic fields generally grow *after* the merger, when the turbulent motions triggered during the merger by the Kelvin-Helmholtz (KH) instability amplify any initial poloidal magnetic field producing a toroidal one whose strength rapidly

becomes comparable to the poloidal one. In addition, we find that magnetic fields can, at least in principle, play a role already *during the inspiral* if sufficiently strong. This is most likely due to the magnetic tension, which decreases the NS deformability, increases the compactness, and thus delays the time of merger. In practice, however, the influence of magnetic fields during the inspiral appears only for values $\sim 10^{17}$ G which are unrealistic (Urpin et al. 1998; Abdolrahimi 2009). As a result, it is very unlikely that present detectors will be able to measure the presence of magnetic fields during the inspiral of NSs. Finally, we show that high-order numerical schemes are essential to draw robust conclusions while lower-order methods incorrectly suggest that even strong magnetic fields have no influence at all.

2 MATHEMATICAL AND NUMERICAL SETUP

All the results presented here were computed by solving the GRMHD equations in the ideal MHD approximation (*i.e.* assuming an infinite electrical conductivity) and in dynamical spacetimes. The evolution of the spacetime was obtained using the CCATIE code, a three-dimensional finite-differencing code providing a solution of a conformally traceless formulation of the Einstein equations (Koppitz et al. 2007; Pollney et al. 2007). The GRMHD equations were instead solved using the Whisky code presented in Giacomazzo & Rezzolla (2007), thus adopting a flux-conservative formulation of the GRMHD equations (Antón et al. 2006) and high-resolution shock-capturing schemes. In particular, we have computed the fluxes using the Harten-Lax-van Leer-Einfeldt (HLL) approximate Riemann solver (Harten et al. 1983), while the reconstruction was made using the 3rd-order piecewise parabolic method (Colella and Woodward 1984). Furthermore, to guarantee the divergence-free character of the MHD equations we have employed the flux-constrained-transport approach (Toth 2000). The code has been validated against a series of tests in special relativity (Giacomazzo & Rezzolla 2006) and in full general relativity [see Giacomazzo & Rezzolla (2007)].

The system of GRMHD equations is closed by an EOS and, as discussed in detail in Baiotti et al. (2008), the choice of the EOS plays a fundamental role in the post-merger dynamics and significantly influences the survival time against gravitational collapse of the hyper-massive neutron star (HMNS) likely produced by the merger. It is hence important that special attention is paid to use EOSs that are physically realistic, as done in Oechslin and Janka (2007) within a conformally-flat description of the fields and a simplified treatment of the hydrodynamics. Because we are here mostly concerned with computing a first quantitative estimate of the role played by magnetic fields rather than with a realistic description of the NS matter, we have employed the commonly used “ideal-fluid” EOS in which the pressure P is expressed as $P = \rho \epsilon (\Gamma - 1)$, where ρ is the rest-mass density, ϵ is the specific internal energy and Γ is the adiabatic exponent. While simple, such EOS provides a reasonable approximation and we expect that the use of realistic EOSs would not change the main results of this work.

All equations are solved on a Cartesian grid using the vertex-centered mesh-refinement scheme provided by the Carpet driver (Schnetter et al. 2004). Differently from Baiotti et al. (2008), we use here larger fixed refined grids rather than smaller moving ones. While computationally more expensive, this choice reduces the violations in the divergence of the magnetic field due to interpolations in the buffer zones between refinement levels. In this way, the divergence of the magnetic field on the finest grid (not including the buffer zones) is zero to machine precision.

We have used five refinement levels with a 180-degree rotational symmetry around the z axis and a reflection symmetry across the $z = 0$ plane (in practice, we simulate only the region $\{x \geq 0, z \geq 0\}$). The finest grid has a resolution of $h = 354.4$ m and extends up to $r = 44$ km; the coarsest grid has $h = 5.6704$ km and extends up to $r = 380$ km. Our finest grid therefore contains both NSs at all times and each NS is covered with $\approx 80^3$ points. In Anderson et al. (2008) the finest grid had $h = 0.46$ km, thus with $\approx 70^3$ points across each star, and Liu et al. (2008) had $\gtrsim 40^3$ points. So our resolution is higher than that in the above works, but it is only half of that in Baiotti et al. (2008), and it is barely sufficient to reach convergent results for the inspiral.

3 INITIAL DATA.

The initial data are the same as used in Baiotti et al. (2008) and were produced by Taniguchi &ourgoulhon (2002) with the multi-domain spectral-method code LORENE (<http://www.lorene.obspm.fr>). The initial solutions for the binaries are obtained assuming a quasi-circular orbit, an irrotational velocity field, and a conformally-flat spatial metric. The matter is modelled using a polytropic EOS $P = K\rho^\Gamma$ with $K = 123.6$ and $\Gamma = 2$. Since no self-consistent solution is available yet for magnetized binaries, a poloidal magnetic field is added a-posteriori using the vector potential $A_\phi \equiv \varpi^2 A_b \max(P - P_{\text{cut}}, 0)^{n_s}$, where $\varpi \equiv \sqrt{x^2 + y^2}$, $A_b > 0$ parameterizes the strength of the magnetic field, P_{cut} defines where in the NS the magnetic field goes to zero, and n_s determines the smoothness of the potential. The components of the magnetic field are then computed by taking the curl of the Cartesian components of A_ϕ to enforce that the divergence of the magnetic field is zero to machine precision. Here we set $P_{\text{cut}} = 0.04 \max(P)$, and $n_s = 2$ to enforce that both the magnetic field and its first derivative are zero at $P = P_{\text{cut}}$. In Anderson et al. (2008) the magnetic field was built with an equivalent expression but with P_{cut} set to the pressure in the atmosphere, and in Liu et al. (2008) the expression used is only slightly different, but P_{cut} is set to be 4% – 0.1% of $\max(P)$. Both above works set $n_s = 1$. Note that the magnetic fields are confined at all times inside the NS matter and hence they cannot “repel” each other during the inspiral, as claimed in Anderson et al. (2008).

Table 1 lists some of the properties of the eight equal-mass binaries studied here. In more detail, we consider two classes of binaries differing in the initial masses, *i.e.* binaries M1.45-B* (or low-mass), and binaries M1.62-B* (or high-mass). For each of these classes we take four different magnetizations (indicated by the asterisk) so that, for instance, M1.45-B12 is a low-mass binary with a maximum initial magnetic field $B_0 = 1.97 \times 10^{12}$ G [the binaries with zero

Table 1. Properties of the eight equal-mass binaries considered.

Binary	B_0 (G)	d/M_{ADM}	M_b (M_\odot)	M_{ADM} (M_\odot)	J ($\text{g cm}^2 \text{s}^{-1}$)	Ω_0 (rad ms^{-1})	r_e (km)	r_p/r_e	ρ_{max} (g cm^{-3})	$(M_*/R)_\infty$
M1.45-B*	0 or $1.97 \times 10^*$	14.3	1.445	2.681	6.5083×10^{49}	1.78	15.2	0.899	4.58×10^{14}	0.12
M1.62-B*	0 or $1.97 \times 10^*$	13.2	1.625	2.982	7.7805×10^{49}	1.85	13.7	0.931	5.91×10^{14}	0.14

Notes. The different columns refer, respectively, to model name; maximum initial magnetic field B_0 , where * is either 0 (in which case $B_0 = 0$), 12, 14 or 17; proper separation between the stellar centres d/M_{ADM} ; baryon mass M_b of each star; total ADM mass M_{ADM} ; angular momentum J ; initial orbital angular velocity Ω_0 ; mean coordinate radius r_e along the line connecting the two stars; ratio of the polar to the equatorial coordinate radii r_p/r_e ; maximum rest-mass density ρ_{max} ; compactness of the stars $(M_*/R)_\infty$.

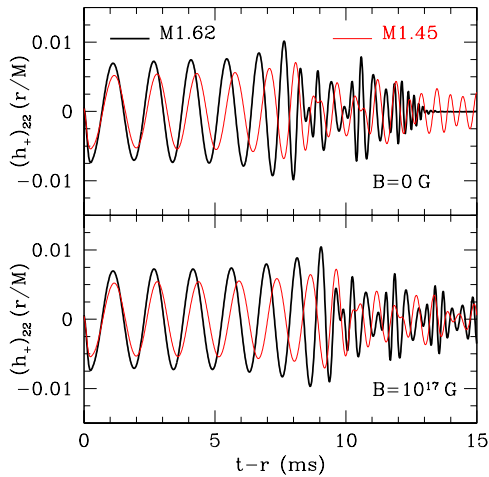


Figure 1. *Top panel:* $\ell = 2$, $m = 2$ component of the h_+ polarization from binaries with different masses (thick line: $1.62 M_\odot$; thin line: $1.45 M_\odot$) and zero magnetic field. *Bottom panel:* the same but for binaries with an initial magnetic field $B_0 \simeq 10^{17}$ G.

magnetic fields are the same as those evolved in Baiotti et al. (2008)]. In summary, we consider 8 different binaries that are either unmagnetized or with magnetic fields as large as $B_0 \simeq 10^{17}$ G. We reinforce a remark already made in the Introduction: all astronomical observations and theoretical considerations suggest that the magnetic fields in binary NS systems just before the merger are much smaller than $\simeq 10^{17}$ G. However, we do consider such large fields here, firstly to compare with those studied by Anderson et al. (2008) and by Liu et al. (2008), and secondly because by doing so we can determine important lower limits on the detectability of magnetic fields during the inspiral.

4 GRAVITATIONAL WAVES AND OVERLAPS

We postpone the discussion on the matter dynamics to a subsequent paper and concentrate here on the GW emission. A representative summary is offered in Fig. 1, which reports the $\ell = 2$, $m = 2$ component of the h_+ polarization (modulo a phase difference, h_\times shows the same behaviour). More specifically, Fig. 1 highlights the differences in the GWs from binaries with different masses, namely $1.62 M_\odot$ (thick line) and $1.45 M_\odot$ (thin line), when the initial magnetic field is either zero (top panel) or as high as $\simeq 10^{17}$ G (bottom panel). Figure 1 clearly shows that when the NSs are not magnetized, the high-mass binary has a larger-amplitude GW emission, it experiences an earlier merger and the HMNS

at these resolutions collapses to a rapidly rotating BH after only ~ 4 ms, while the HMNS from the low-mass binary does not collapse. In contrast, when the NSs are initially magnetized, the strong magnetic tension most likely reduces the tidal deformations and results in a delayed merger time (defined as the time when the maximum rest-mass density has a first significant minimum; cf. Fig 2 or 8 in Baiotti et al. (2008)). Furthermore, the additional pressure support coming from the intense magnetic fields is such that neither the high-mass nor the low-mass binary collapse promptly to a BH over the ~ 15 ms of the simulations (see the bottom panel of Fig. 4 for a comparison of GWs for high-mass binaries with different magnetic fields). Overall, Fig. 1 shows that magnetic fields have a strong impact on the GWs emitted after the merger but *also* during the inspiral, if sufficiently strong. If, on the other hand, the magnetic fields are more realistic, e.g. $\sim 10^{12}$ G, then differences appear *only* after the merger. For compactness, comparisons of this type cannot be presented here but will appear in a longer companion paper (Baiotti et al., in preparation).

While generic, this behaviour depends sensitively on the strength of the initial magnetic field and there exists a critical magnetic field below which the MHD effects during the inspiral are not important. In order to quantify this we have computed the overlap between two waveforms h_{B_1} , h_{B_2} from binaries with initial magnetic fields B_1 , B_2 as

$$\mathcal{O}[h_{B_1}, h_{B_2}] \equiv \frac{\langle h_{B_1} | h_{B_2} \rangle}{\sqrt{\langle h_{B_1} | h_{B_1} \rangle \langle h_{B_2} | h_{B_2} \rangle}}, \quad (1)$$

where $\langle h_{B_1} | h_{B_2} \rangle$ is the scalar product and is defined as

$$\langle h_{B_1} | h_{B_2} \rangle \equiv 4\Re \int_0^\infty df \frac{\tilde{h}_{B_1}(f) \tilde{h}_{B_2}^*(f)}{S_h(f)}, \quad (2)$$

and $\tilde{h}(f)$ is the Fourier transform of the GW $h(t)$ and $S_h(f)$ is the noise power spectral density of the detector (we have here considered LIGO). Clearly, waveforms that are very similar have $\mathcal{O} \simeq 1$. A general view is shown in Fig. 2, which reports the overlaps between the unmagnetized binaries and binaries with different magnetizations, *i.e.* $\mathcal{O}[h_{B_0}, h_B]$, for the two masses considered here (top and bottom panels, respectively). Note that the overlap is relative to the inspiral only [*i.e.* the integral (2) is cut off at the orbital frequency at merger] since this is the phase for which our results are convergent (becoming only consistent after the merger as a result of the development of turbulence) and because the post-merger evolution can only further decrease \mathcal{O} . It is evident that for the high-mass binary (top panel) the influence of the magnetic field is noticeable only for very large magnetic fields ($\mathcal{O} \simeq 0.999$ for $B_0 \simeq 10^{14}$ G and $\mathcal{O} \simeq 0.668$ for $B_0 \simeq 10^{17}$ G). This is true also for the low-mass binary (bottom panel) whose smaller compactness, however, leads

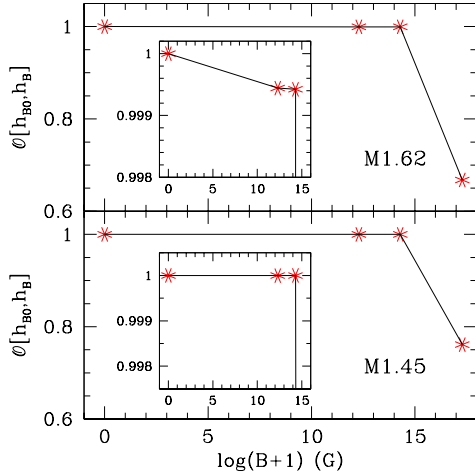


Figure 2. Overlap in inspiral waveforms from binaries with different magnetization; the top and bottom panels refer to the high- and low-mass binaries, respectively.

to larger overlaps (*i.e.* $\mathcal{O} \simeq 0.761$ for $B_0 \simeq 10^{17}$ G). In view of these results, of the fact that NSs just prior to merger are expected to have magnetic fields $\sim 10^8 - 10^{10}$ G (Urpin et al. 1998; Abdolrahimi 2009), and that present detectors are sensitive to $\mathcal{O} \lesssim 0.995$ (Lindblom et al. 2008), we conclude that it is very unlikely that the presence of realistic magnetic fields can be detected during the inspiral.

5 MAGNETIC FIELD AMPLIFICATION

As discussed in detail in Baiotti et al. (2008), during the merger a shear layer develops in the region where the two NSs enter in contact. Across this layer, the tangential components of the velocity are discontinuous and this leads to the development of a KH instability and thus to the production of vortices [*cf.* Fig. 16 of Baiotti et al. (2008)]. When poloidal magnetic fields are present, this hydrodynamical instability can lead to exponentially growing toroidal magnetic fields, thus increasing the energy stored in magnetic fields. This mechanism, already observed in Newtonian simulations (Price and Rosswog 2006) but not before in general relativistic ones, is likely to be important for explaining the physics powering short GRBs. Taking M1.62-B12 as a reference, Fig. 3 shows the evolution of the maxima of the magnetic field $|B| \equiv (B^i B_i)^{1/2}$ (thick line), and of its toroidal $|B^T|$ (dashed line), and poloidal $|B^P|$ (thin line) components. A vertical dotted line marks the merger, occurring ≈ 1 ms after the KH instability has started developing. Clearly, as long as the KH instability is active, the toroidal magnetic field is amplified exponentially, until it reaches values comparable to the poloidal one (this is different and more reasonable than what found by Price and Rosswog (2006), where the magnetic field reached energy equipartition values). Note that the magnetic field grows considerably also when the HMNS collapses to a BH as a result of magnetic-flux conservation in the collapsing NS matter.

As discussed in Price and Rosswog (2006) and in Baiotti et al. (2008), much in the development of the

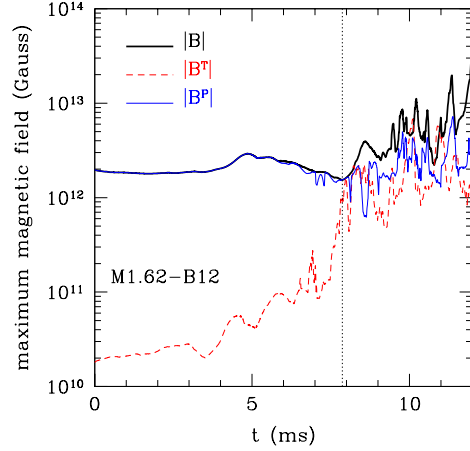


Figure 3. Evolution of the maxima of the magnetic field $|B| \equiv (B^i B_i)^{1/2}$ (thick solid line) and of its toroidal $|B^T|$ (dashed line) and poloidal $|B^P|$ (thin solid line) components for the high-mass case with $B_0 \simeq 10^{12}$ G. The dotted line marks the merger time.

KH instability and in the subsequent magnetic field amplification depends on the resolution used. A detailed study of the turbulent regime and magnetic field amplification produced by the merger is extremely challenging and requires resolutions well above the ones that can be afforded now in GRMHD simulations. Nevertheless, on the basis of preliminary investigations with different resolutions, we expect the behaviour in Fig. 3 to be qualitatively correct and, hence, that as long as the KH is active, the poloidal magnetic field is coiled into a toroidal one, increasing it exponentially to values comparable with the poloidal one. When equipartition among the components is reached, the large magnetic tension suppresses the KH instability, preventing a further growth of the toroidal magnetic field. An analysis of this process will be presented elsewhere.

6 THE IMPORTANCE OF HIGH-ORDER METHODS

As shown in Baiotti et al. (2008), the use of reconstruction schemes of sufficiently high order is *essential* for a correct calculation of the GW signal. This is stressed also in Fig. 4, which presents a comparison in the GW emission from the high-mass binary for evolutions made using either a 2nd-order MINMOD scheme (top panel) or a 3rd-order PPM one (bottom panel) with the same grid structure and resolution used in the previous runs. In both cases a thick line refers to the unmagnetized binary while a thin line to the binary with $B_0 \simeq 10^{17}$ G. Clearly, while the evolutions with MINMOD show only minimal differences between the magnetized and unmagnetized case ($\mathcal{O} = 0.9994$ over the whole waveform), the evolutions using PPM show considerable differences ($\mathcal{O} = 0.6500$), both during the inspiral and after the merger. More precisely, although we use exactly the same initial data, the binaries evolved with MINMOD merge almost two orbits earlier than those evolved with PPM [*cf.* vertical dotted lines in Fig. 4]. Additionally, the unmagnetized binary evolved with MINMOD does not

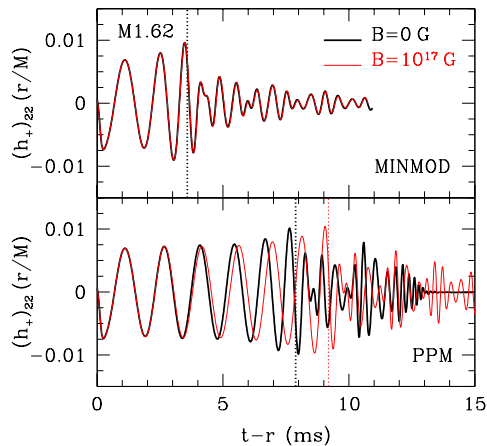


Figure 4. GW emission from the the high-mass binary evolved using either a 2nd-order scheme (top panel) or a 3rd-order one (bottom panel). A thick (thin) line refers to a binary with $B_0 = 0$ G (10^{17} G), while the vertical lines indicate the time of merger.

collapse to a BH, in contrast to what happens when using PPM at these resolutions. These differences are due to the numerical dissipation of the 2nd-order method, which is inadequate at these resolutions. This could explain why the calculations in Liu et al. (2008), where a 2nd-order reconstruction and a lower resolution were used, show only small differences between unmagnetized and magnetized binaries.

7 CONCLUSIONS

We have presented accurate simulations of the inspiral and merger of magnetized NSs and found that magnetic fields have an impact *both* during the inspiral and after the merger but only if sufficiently strong. Comparing waveforms for different magnetizations we have found that for $B_0 \lesssim 10^{14}$ G, the overlap $\mathcal{O} \gtrsim 0.999$ and is quite insensitive to the mass of the NSs. Only for unrealistically large magnetic fields ($B_0 \simeq 10^{17}$ G), the overlap decreases noticeably, becoming at our resolutions $\mathcal{O} \lesssim 0.76/0.67$ for stars with baryon masses $M_b \simeq 1.4/1.6 M_\odot$, respectively. Since the magnetic fields in NSs just prior to merger are expected to be rather small ($\sim 10^8 - 10^{10}$ G) (Urpin et al. 1998; Abdolrahimi 2009), we conclude that it is very unlikely that the present detectors will be able to measure the presence of magnetic fields during the inspiral. Magnetic fields could be however detectable after the merger and hence in the part of the spectrum at frequencies $\gtrsim 2$ kHz [*cf.* spectra in Baiotti et al. (2008)].

Another important result discussed here is the evidence that a KH instability develops during the merger, leading to the exponential growth of a toroidal magnetic field, the strength of which becomes comparable with the poloidal one. This additional magnetic field can modify the structure of the HMNS and decrease the overlap after the merger. Finally, we have provided concrete evidence that high-order methods are *essential* to draw robust conclusions and that instead lower-order methods incorrectly suggest that magnetic fields have no influence at all.

ACKNOWLEDGMENTS

We thank the developers of *Lorene* for the initial data and those of *Carpet* for the mesh refinement. Special thanks go to our late colleague and friend Thomas Radke. Useful input from C. Palenzuela, D. Neilsen, J. Read, C. Reisswig, M. Ruffert (who acted as referee), L. Santamaria, E. Schnetter, A. Tonita, and S. Yoshida is also acknowledged. The computations were performed at the AEI and at LONI. This work is also supported by the DFG SFB/Transregio 7 and by the JSPS grant 19-07803.

REFERENCES

- Abdolrahimi S., arXiv:0905.0229 (2009)
- Anderson M., Hirschmann E. W., Lehner L., Liebling S. L., Motl P. M., Neilsen D., Palenzuela C. and Tohline J. E., Phys. Rev. Lett. 100, 191101 (2008)
- Antón L., Zanotti O., Miralles J. A., Martí J. M., Ibáñez J. M., Font J. A. and Pons J. A., Astrophys. J. 637, 296 (2006)
- Baiotti L., Giacomazzo B. and Rezzolla L., Phys. Rev. D 78, 084033 (2008)
- Colella P. and Woodward P. R., J. Comput. Phys. 54, 174 (1984)
- Giacomazzo B. and Rezzolla L., Journal of Fluid Mechanics 562, 223 (2006)
- Giacomazzo B. and Rezzolla L., Class. Quantum Grav. 24, S235 (2007)
- Harten A., Lax P. D. and van Leer B., SIAM Rev. 25, 35 (1983)
- Koppitz M., Pollney D., Reisswig C., Rezzolla L., Thornburg J., Diener P. and Schnetter E., Phys. Rev. Lett. 99, 041102 (2007)
- Lindblom L., Owen B. J. and Brown D. A., Phys. Rev. D 78, 124020 (2008)
- Liu Y. T., Shapiro S. L., Etienne Z. B. and Taniguchi K., Phys. Rev. D 78, 024012 (2008)
- Meszaros P., Rept. Prog. Phys. 69, 2259 (2006)
- Oechslin R. and Janka H. T., Phys.Rev.Lett. 99, 121102 (2007)
- Piran T., Rev. Mod. Phys. 76, 1143 (2004)
- Pollney D., Reisswig C., Rezzolla L., Szilágyi B., Ansorg M., Deris B., Diener P., Dorband E. N., Koppitz M., Nagar A., et al., Phys. Rev. D 76, 124002 (2007)
- Price R. H. and Rosswog S., Science 312, 719 (2006)
- Read J. S., Markakis C., Shibata M., Uryu K., Creighton J. D. E. and Friedman J. L., Phys. Rev. D 79, 124033 (2009)
- Schnetter E., Hawley S. H. and Hawke I., Class. Quantum Grav. 21, 1465 (2004)
- Taniguchi K. and Gourgoulhon E., Phys. Rev. D 66, 104019 (2002)
- Toth G., J. Comput. Phys. 161, 605 (2000)
- Urpin, V. and Geppert, U. and Konenkov, D., MNRAS, 295, 907 (1998)
- Yamamoto T., Shibata M. and Taniguchi K., Phys. Rev. D 78, 064054 (2008)